Analysis of Plasmon Resonance in a Multilayer-coated Bigrating

Xun Xu[1], **Yoichi Okuno**[2], **and Taikei Suyama**[3]

[1]Kyushu Sangyo University, Fukuoka, Japan
[2]South China Normal University, Guangzhou, China
[3]Akashi National College of Technology, Akashi, Japan

Abstract— Periodically corrugated thin metal films have an interesting property such as the partial or total resonance absorption of incident light energy. The resonance absorption is associated with the excitation of the surface plasmons and is then termed the resonance absorption. Most of studies on the resonance absorption have mainly dealt with a thin metal film grating whose surfaces are periodic in one direction. We investigate the plasmon resonance of a multilayer-coated bigrating which consists of thin-films corrugated periodically in two directions. In solving the problem, we employed a computational technique based on modal expansion. Taking a sandwiched structure Vacuum/Ag/SiO_2/Ag/Vacuum for an example, we observed: (1) excitation of a SISP mode at the lit surface of the 1st Ag layer with strong field enhancement for thick enough Ag layer case; (2) excitation of coupled SPR modes (SRSP or LRSP) at each surface between vacuum and Ag layers with strong field enhancements for thin enough Ag layer cases no matter with the thickness of SiO_2 layers; (3) standing wave pattern of the electric filed in the SiO_2 film. The coupled plasmon modes were resulted by the resonance waves excited on four surfaces in these cases.

1. INTRODUCTION

In our previous study we examined the excitation of coupled plasmon modes in a thin-film grating made of a metal [1]. When the metal is thick, e.g., more than ten times the skin depth, the plasmon can be excited on the lit surface alone. This is termed a single-interface surface plasmon (SISP). When the thickness is decreased, the plasmon can be seen also on the other surface of the film. The two plasmon waves interact with each other to form coupled plasmon modes called short-range and long-range surface plasmon (SRSP and LRSP) [2].

In the present research we consider a sandwiched structure: metal/dielectric/metal, which is interesting for a wide area of applications including biosensors [3].

2. FORMULATION AND METHOD OF SOLUTION

In this section we first formulate the problem of diffraction by multilayered bigratings shown in Fig. 1(a). After formulating the problem we state a method of solution based on a modal-expansion approach.

2.1. Incident Wave

The electric and magnetic field of an incident light are given by

$$\begin{bmatrix} \mathbf{E}^i \\ \mathbf{H}^i \end{bmatrix} (\mathbf{P}) = \begin{bmatrix} \mathbf{e}^i \\ \mathbf{h}^i \end{bmatrix} \exp(i\mathbf{k}^i \cdot \mathbf{P}) \tag{1}$$

where $\mathbf{e}^i$ and $\mathbf{h}^i$ are the electric- and magnetic-field amplitude; $\mathbf{k}^i = [\alpha, \beta, -\gamma]$ is the incident wavevector with $\alpha = n_1 k \sin\theta \cos\varphi$, $\beta = n_1 k \sin\theta \sin\varphi$, $\gamma = n_1 k \cos\theta$, $k = 2\pi/\lambda$ and n_1 is the relative refractive index of region V_1; $\mathbf{P} = (\ X,\ Y,\ Z)$ is an observation point; λ is the wavelength of the incident wave; θ is the incident angle between the Z-axis and the incident wave-vector; and φ is the azimuth angle between the X-axis and the plane of incidence.

The amplitude of the incident electric field can be decomposed into TE- and TM component, which means the electric (or magnetic) field is perpendicular to the plane of incidence. To do this, we define two unit vectors $\mathbf{e}^{\mathrm{TE}}$ and $\mathbf{e}^{\mathrm{TM}}$ that span a plane orthogonal to $\mathbf{k}^i$. Hence, the amplitude $\mathbf{e}^i$ in (3) is decomposed as

$$\mathbf{e}^i = \mathbf{e}^{\mathrm{TE}} \cos\delta + \mathbf{e}^{\mathrm{TM}} \sin\delta \tag{2}$$

where δ is the polarization angle between $\mathbf{e}^i$ and $\mathbf{e}^{\mathrm{TE}}$ as shown in Fig. 1(b).

2.2. Diffracted Wave

We seek for the diffracted fields $\mathbf{E}_\ell(\mathbf{P})$ and $\mathbf{H}_\ell(\mathbf{P})$ in each region, i.e., $\ell = 1, 2, \ldots, L+1$. They should satisfy the following requirements:

(C1) The Helmholtz equations in each region;

(C2) Radiation conditions: The diffracted waves in V_1 (or V_{L+1}) should propagate or attenuate in the positive (or negative) Z-direction;

(C3) Periodicity conditions: Each component of the diffracted electric and magnetic field should satisfy

$$f\left(X+d_X, Y, Z\right) = \exp\left(i\alpha d_X\right) f\left(X, Y, Z\right) \tag{3}$$

$$f\left(X, Y+d_Y, Z\right) = \exp\left(i\beta d_Y\right) f\left(X, Y, Z\right) \tag{4}$$

where α and β are the phase constants in X and Y.

(C4) Boundary conditions: The tangential components of electric and magnetic fields are continuous across the boundaries S_ℓ $(\ell = 1, 2, \ldots, L+1)$.

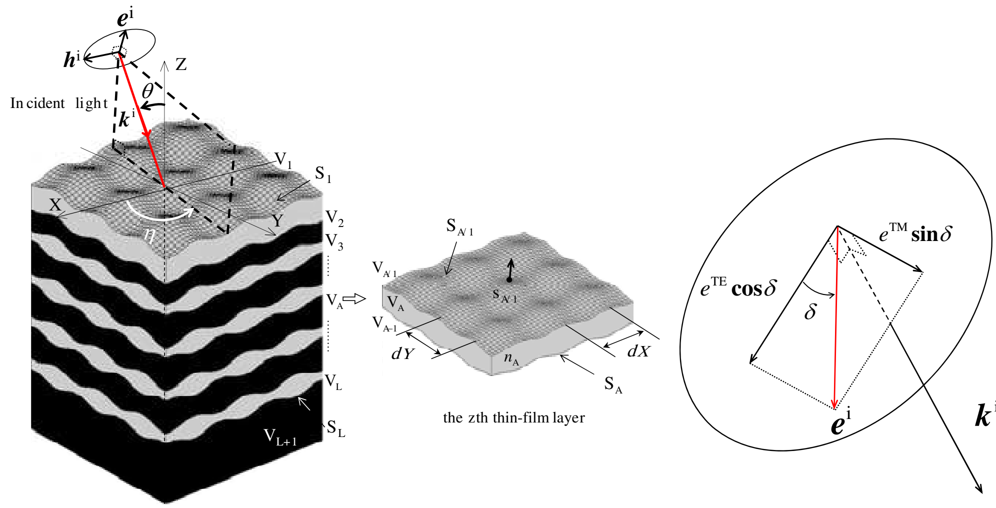

Figure 1: (a) Schematic representation of a multilayered bigrating with an incident light (V_1: $\{\mathbf{P}|Z > S_1(X,Y)\}$, V_{L+1} : $\{\mathbf{P}|Z < S_L(X,Y)\}$); (b) Definition of a polarization angle.

2.3. Method of Solution

We solve the problem above using Yasuura's method of modal expansion [4, 5]. To do this, we first define the sets of modal functions; next we construct approximate solutions in terms of finite modal expansions with unknown coefficients; and, finally we determine the coefficients applying the boundary conditions.

Modal functions: Because the diffracted waves have both TE- and TM-components, we need TE and TM vector modal functions in constructing the solutions. Here we employ the functions derived from the Floquet modes (separated solutions of the Helmholtz equations satisfying the periodicity (C3) and the radiation conditions (C2) if necessary). The modal functions for electric fields for each region are given by

$$\boldsymbol{\varphi}_{\ell mn}^{\mathrm{TE,TM}\pm}(\mathbf{P}) = \mathbf{e}_{\ell mn}^{\mathrm{TE,TM}\pm} \exp(i\mathbf{k}_{\ell mn}^{\pm} \cdot \mathbf{P}) \tag{5}$$

where, $m, n = 0, \pm 1, \pm 2, \ldots$, $\ell = 1, 2, \ldots, L+1$, and unit vectors $\mathbf{e}$ in (5) are defined by

$$\mathbf{e}_{\ell mn}^{\mathrm{TE}\pm} = \frac{\mathbf{k}_{\ell mn}^{\pm} \times \mathbf{i}_Z}{\left|\mathbf{k}_{\ell mn}^{\pm} \times \mathbf{i}_Z\right|}, \quad \mathbf{e}_{\ell mn}^{\mathrm{TM}\pm} = \frac{\mathbf{e}_{\ell mn}^{\mathrm{TE}\pm} \times \mathbf{k}_{\ell mn}^{\pm}}{\left|\mathbf{e}_{\ell mn}^{\mathrm{TE}\pm} \times \mathbf{k}_{\ell mn}^{\pm}\right|} \tag{6}$$

and

$$\mathbf{k}_{\ell mn}^{\pm} = \left[\alpha_m, \beta_n, \pm\gamma_{\ell mn}\right], \quad \alpha_m = \alpha + \frac{2m\pi}{d_x}, \ \beta_n = \beta + \frac{2n\pi}{d_y}, \quad \gamma_{\ell mn} = \left(n_\ell^2 k^2 - \alpha_m^2 - \beta_n^2\right)^{1/2} \tag{7}$$

where $\mathrm{Re}(\gamma_{\ell mn}) \geq 0$ and $\mathrm{Im}(\gamma_{\ell mn}) \geq 0$. We use the modal functions defined in equations from (5) to (7) to construct approximations of diffracted electric fields. For the accompanying magnetic fields, we employ

$$\boldsymbol{\psi}_{\ell mn}^{\mathrm{TE,TM}\,\pm}(\mathbf{P}) = \frac{1}{\omega\mu_0}\mathbf{k}_{\ell mn}^{\pm} \times \boldsymbol{\varphi}_{\ell mn}^{\mathrm{TE,TM}\,\pm}(\mathbf{P}). \tag{8}$$

Approximate solutions: To satisfy the radiation condition (C2), the approximate solution in V_1 should have a form of finite linear combination of up-going modal functions with unknown coefficients. Likewise, the solution in V_{L+1} must be a linear combination of down-going modal functions. The solution in V_ℓ, however, must have both up- and down-going waves. To show the travelling direction of a modal function, we use superscripts + and − representing up- and down-going waves. Here, we form approximate solutions for the diffracted electric and magnetic fields in V_ℓ:

$$\begin{aligned}\begin{pmatrix} E_{\ell N}^{d} \\ H_{\ell N}^{d} \end{pmatrix}(\mathbf{P}) = & \sum_{m,n=-N}^{N} A_{\ell mn}^{TE+}(N) \begin{pmatrix} \varphi_{\ell mn}^{TE+} \\ \psi_{\ell mn}^{TE+} \end{pmatrix}(\mathbf{P}) + \sum_{m,n=-N}^{N} A_{\ell mn}^{TM+}(N) \begin{pmatrix} \varphi_{\ell mn}^{TM+} \\ \psi_{\ell mn}^{TM+} \end{pmatrix}(\mathbf{P}) \\ & + \sum_{m,n=-N}^{N} A_{\ell mn}^{TE-}(N) \begin{pmatrix} \varphi_{\ell mn}^{TE-} \\ \psi_{\ell mn}^{TE-} \end{pmatrix}(\mathbf{P}) + \sum_{m,n=-N}^{N} A_{\ell mn}^{TM-}(N) \begin{pmatrix} \varphi_{\ell mn}^{TM-} \\ \psi_{\ell mn}^{TM-} \end{pmatrix}(\mathbf{P}) \\ & (\ell = 1, 2, \ldots, L+1) \end{aligned} \tag{9}$$

where N denotes the number of truncation.

Boundary matching: Because the approximate solutions satisfy the requirements (C1), (C2), and (C3) by definition, the unknown coefficients $A_{\ell mn}^{\mathrm{TE}\pm}(N)$ and $A_{\ell mn}^{\mathrm{TM}\pm}(N)$ are determined such that the solutions satisfy the boundary conditions (C4) in an approximate sense. In the Yasuura's method [4], the least-squares method is employed to fit the solution to the boundary conditions. That is, we find the coefficients that minimize the weighted mean-square error by

$$\begin{aligned} I_N = & \int_{\mathrm{S}'_\ell} \left|\boldsymbol{v} \times \left[\mathbf{E}_{1N}^{\mathbf{d}} + \mathbf{E}^{i} - \mathbf{E}_{2N}^{\mathbf{d}}\right](s_1)\right|^2 \mathbf{d}s_1 + |\Gamma_1|^2 \int_{\mathrm{S}'_\ell} \left|\boldsymbol{v} \times \left[\mathbf{H}_{1N}^{\mathbf{d}} + \mathbf{H}^{i} - \mathbf{H}_{2N}^{\mathbf{d}}\right](s_1)\right|^2 \mathbf{d}s_1 \\ & + \sum_{\ell=2}^{L} \left\{ \int_{\mathrm{S}'_\ell} \left|\boldsymbol{v}\times\left[\mathbf{E}_{\ell N}^{\mathbf{d}} - \mathbf{E}_{\ell+1,N}^{\mathbf{d}}\right](s_\ell)\right|^2 \mathbf{d}s_\ell + |\Gamma_\ell|^2 \int_{\mathrm{S}'_\ell} \left|\boldsymbol{v} \times \left[\mathbf{H}_{\ell N}^{\mathbf{d}} - \mathbf{H}_{\ell+1,N}^{\mathbf{d}}\right](s_\ell)^2\right| \mathbf{d}s_\ell \right\} \end{aligned} \tag{10}$$

where S'_ℓ denotes one-period cells of the interface S_ℓ, Γ_ℓ is the intrinsic impedance of the medium in V_ℓ and $\boldsymbol{v}$ is a unit normal vector of each boundary.

To solve the least-squares problem on a computer, we need a discretized form of the problem. We first discretize the weighted mean-square error I_N by applying a two-dimensional trapezoidal rule where the number of sampling points is chosen as $2(2N+1)$ [5, 6]. We then employ orthogonal decomposition methods [singular-value decomposition (SVD) and QR decomposition (QRD)] in solving the discretized problem [6].

3. NUMERICAL RESULTS

The multilayered bigrating is composed of three layers: Ag/$\mathrm{SiO_2}$/Ag. The incident light is a TM-polarized plane wave with a 650 nm wavelength. The relative refractive index of vacuum is 1, $n_{\mathrm{Ag}} = 0.07 + 4.2\mathrm{i}$ and $n_{\mathrm{SiO_2}} = 1.5$. The periods are set to be $d_x = d_y = 556\,\mathrm{nm}$. We consider three types of grating with different thickness pairs of each region: (A) $e_{\mathrm{Ag}} = e_{\mathrm{SiO_2}} = 27.8\,\mathrm{nm}$; (B) $e_{\mathrm{Ag}} = 27.8\,\mathrm{nm}$, $e_{\mathrm{SiO_2}} = 278\,\mathrm{nm}$; and (C) $e_{\mathrm{Ag}} = 278\,\mathrm{nm}$ $e_{\mathrm{SiO_2}} = 27.8\,\mathrm{nm}$. We show the diffraction efficiency and field distributions of these gratings below.

Figure 2 shows the (0, 0)-th order reflection and transmission efficiency as functions of the incident angle θ for the three types of grating with the azimuth angle is set to be $\varphi = 45°$.

Five dips are observed on the reflection curves throughout Figs. 2(a)–2(c). In type (A) shown in Fig. 2(a), two dips (dip 1 at $\theta = 10.6°$ and dip 2 at $\theta = 12.5°$) are observed; at the same points the transmission efficiency has small peaks. This shows that the plasmon surface wave is excited on the four surfaces of Ag films; and the surface wave at the bottom surface excites a propagating mode in V_5. These surface waves are coupled modes SRSP or LRSP [1].

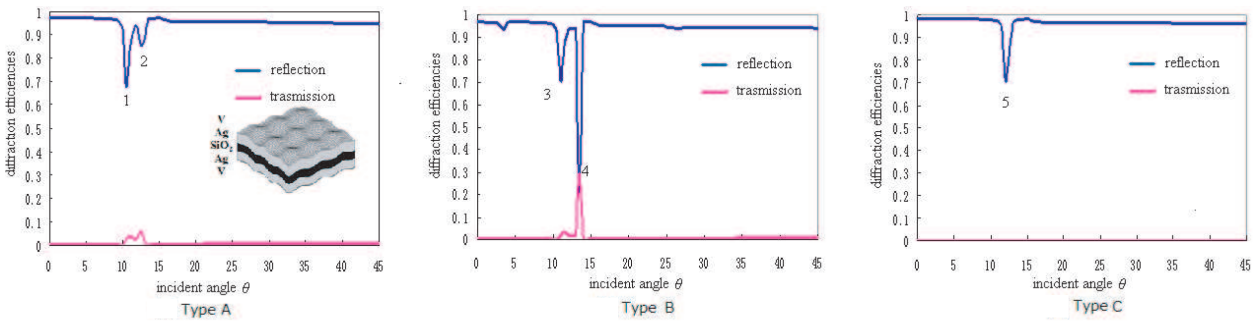

(a) (b) (c)

Figure 2: The (0, 0)-th order reflection and transmission efficiency for 3-layered doubly periodic gratings (a) $e_{\mathrm{Ag}} = e_{\mathrm{SiO_2}} = 27.8\,\mathrm{nm}$; (b) $e_{\mathrm{Ag}} = 27.8\,\mathrm{nm}$, $e_{\mathrm{SiO_2}} = 278\,\mathrm{nm}$; and (c) $e_{\mathrm{Ag}} = 278\,\mathrm{nm}$, $e_{\mathrm{SiO_2}} = 27.8\,\mathrm{nm}$.

For type (B) shown in Fig. 2(b), two dips (dip 3 at $\theta = 11.1°$ and dip 4 at $\theta = 13.5°$) are observed on reflection curve and the transmission coefficient increases at the same time. Reflection at dip 4 is much lower than that of dips 1 and 2 accompanying change of the thickness of SiO_2. The coupled plasmon modes are resulted by resonance waves excited at four surfaces [1].

In type (C) shown in Fig. 2(c), only one dip (dip 5 at $\theta = 12.0°$) is observed on reflection curve and no transmission can be seen. This shows excitation of SISP [1].

Next, we investigated the field distributions of the total electric field E^{total} and the TM component of the (0, 0)th-order diffracted electric field $E^{\mathrm{TM}}_{\ell(0,0)}$ in the vicinity of the SiO_2 film. The magnitude of E^{total} and $E^{\mathrm{TM}}_{\ell(0,0)}$ $(\ell = 1,\ 2,\ \cdots,\ 5)$ along the Z-axis are plotted in Fig. 3 where $\theta = 0°$ and $e_{\mathrm{SiO_2}} = 166.8\,\mathrm{nm}$. We observe in the figure that the field distributions of E^{total} inside the SiO_2 film indicates a standing wave pattern corresponding to the normal mode of a onedimensional cavity resonator, and that the distribution is almost close to that of $E^{\mathrm{TM}}_{3(0,0)}$. We think that the field distribution is associated with resonance of the (0, 0)th-order diffracted wave $E^{\mathrm{TM}}_{3(0,0)}$ in the SiO_2 film sandwiched by a silver film grating.

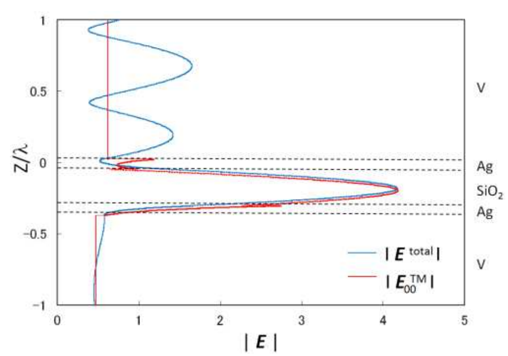

Figure 3: Standing wave pattern of the electric filed in the SiO_2 film.

4. CONCLUSIONS

We solved the problems for 3-layered bigratings. By calculating the diffraction efficiency and field distributions, we observed: (1) excitation of a SISP mode at the lit surface of the 1st Ag layer with strong field enhancement for a thickenough Ag layer case; (2) excitation of coupled SPR modes (SRSP or LRSP) at each surface between vacuum and Ag layers with strong field enhancements for thin enough Ag layer cases no matter with the thickness of SiO_2 layers; (3) standing wave pattern of the electric filed in the SiO_2 film. The coupled plasmon modes were resulted by the resonance waves excited on four surfaces in these cases We are planning to study the nature of the plasmon surface waves excited on the multilayered thin metal/dielectric gratings.

REFERENCES

1. Suyama, T, A. Matsushima, Y. Okuno, and T. Matsuda, "Resonant excitation of plasmons in bigrating," *Plasmonics — Principles and Applications*, K. Kim (Ed.), Chap. 12, 313–334, INTECH, Rijeka, 2012.
2. Hibbins, A. P., W. A. Murray, J. Tyler, S. Wedge, W. L. Barnes, and J. R. Sambles, "Resonant absorption of electromagnetic fields by surface plasmons buried in a multilayered plasmonic nanostructure," *Phys. Rev. B*, Vol. 74, No. 073408, 2006.
3. Ahn, J. H., T. Y. Seong, W. M. Kim, T. S. Lee, I. Kim, and K. S. Lee, "Fiber-optic waveguide coupled surface plasmon resonance sensor," *Optics Express*, Vol. 20, No. 19, 21729–21738, 2012.
4. Okuno, Y., "Mode-matching Method," *Analysis Methods for Electromagnetic Wave Problems*, E. Yamashita (Ed.), 107–138, Artech House, Boston, 1990
5. Yasuura, K. and T. Itakura, "Approximation method for wave functions (I), (II), and (III)," *Kyushu Univ. Tech. Rep.*, Vol. 38, 72–77, 1965; Vol. 38, 378–385, 1966; Vol. 39, 51–56, 1966.
6. Matsuda, T. and Y. Okuno, "Numerical evaluation of plane-wave diffraction by a doubly periodic grating," *Radio Sci.*, Vol. 31, 1791–1798, 1996.